

RESEARCH ARTICLE

 OPEN ACCESS

Received: 21.12.2020

Accepted: 25.02.2021

Published: 07.05.2021

Citation: Karimi AK, Uchida R, Aasim BA, Tomiyama J, Suda Y (2021) Numerical study on the temporal changes of the principal stresses at the ends of the hollow PC-girders to control horizontal end cracks. Indian Journal of Science and Technology 14(16): 1283-1295. <https://doi.org/10.17485/IJST/v14i16.2280>

* **Corresponding author.**karimi@kdru.edu.af**Funding:** None**Competing Interests:** None

Copyright: © 2021 Karimi et al. This is an open access article distributed under the terms of the [Creative Commons Attribution License](https://creativecommons.org/licenses/by/4.0/), which permits unrestricted use, distribution, and reproduction in any medium, provided the original author and source are credited.

Published By Indian Society for Education and Environment ([iSee](https://www.indst.org/))

ISSN

Print: 0974-6846

Electronic: 0974-5645

Numerical study on the temporal changes of the principal stresses at the ends of the hollow PC-girders to control horizontal end cracks

Abdul Khaliq Karimi^{1,2*}, Ryota Uchida³, Bashir Ahmad Aasim^{1,2}, Jun Tomiyama⁴, Yuya Suda⁵

1 Ph.D. Scholar, Department of Civil Engineering, University of the Ryukyus, Okinawa, Japan

2 Civil Engineering Department, Kandahar University, Kandahar, Afghanistan

3 FUJI P.S Corporation, Kyusyu Kotake Factory, Kyusyu, Japan

4 Professor, Department of Civil Engineering, University of the Ryukyus, Okinawa, Japan

5 Assistant Professor, Department of Civil Engineering, University of the Ryukyus, Okinawa, Japan

Abstract

Background/Objectives: To professionally meet bridge load demands, hollow PC-girders are recently considered for bridge construction, particularly in Japan. Hollow girders are pretensioned girders, which can be a good alternative for ordinary PC-girders by having lightweight, using less material than other beams, and spanning long distances. Hollow PC-girders can be vulnerable to horizontal end cracking at the time of prestressing strand release. **Methods:** In this study, a nonlinear finite element analysis was performed to investigate the occurrence of horizontal cracks at the time of prestressing at the ends of hollow PC-girders. First, the selected hollow girder was miniaturized to a span length of 4 m required for sufficiently prestressing; then, a standard static prestressing analysis was performed using a finite element analysis software Midas FEA. This software is an analysis tool with standard FEM analysis functions in the construction field and can perform detailed analysis for reinforcements and concrete crack analysis. The software was used to model the girder and investigate the temporal changes of principal stresses at hollow PC-girders' ends. **Findings:** The study showed that placing only end-zone reinforcements cannot reduce principal stresses to the level to be less than the concrete's tensile strength. However, debonding four PC-strands at the ends of the girder alongside the placement of end-zone reinforcements could sufficiently reduce principal stresses to the level to be less than the tensile strength of concrete, and consequently, horizontal cracks were eliminated at the ends of the hollow PC-girder.

Keywords: Horizontal cracks; pretensioned girders; hollow PCgirders; finite element analysis; Midas FEA

1 Introduction

In the 1930s, with the advent of the prestressed concrete industry by French engineer Eugene Freyssinet⁽¹⁾, high strength concrete and high strength steel became economically usable. Prestressed concrete may crack when a force exceeding the design load is applied, but once the force removes it has high resilience, the crack closes to return to the original state again. Thus, prestressed concrete is using for many years in bridge construction. To meet the bridge load demands effectively, pretensioned PC-girders are prestressed heavily in most cases⁽²⁾. In the end regions of a PC-girder where the prestressing applies, horizontal cracks occur during or immediately after prestressing. Several possible sources may increase or decrease the likelihood of horizontal cracking at the ends of pretensioned girders: method of detensioning, the release of the top straight or draped strands before the bottom straight strands, the order of release of bottom strands with the flame cutting method, length of the free strand in the prestressing bed, friction with the bottom form of the prestressing bed, heat concentration during flame cutting, lifting the precast member from the bed, Hoyer effect, use of large strands, unacceptable design of end zone reinforcement, concrete type, low concrete release strength, and strand distribution^(3–10).

Deeper girders with larger prestressing forces tend to have more, longer, and broader cracks⁽¹¹⁾. If end zones are not kept from the horizontal crack occurrence, it may create corrosion concerns⁽²⁾. It was founded around the 1960s; horizontal cracks occur in the pretensioned member ends, Marshall and Mattock⁽¹²⁾ investigated with an experimental study. After that, multiple researchers have done analytical studies (such as the Gergely-Sozen model, strut-and-tie models, and nonlinear finite element analysis) and experimental studies to realize the end-zone stresses or to design the end-zone reinforcements^(5–8,11,13–18).

Hollow girders are incredibly vulnerable to horizontal end cracking amongst the PC-girders⁽¹⁹⁾ because they are hollow inside along the beam's length except for the few transverse diaphragms which stiffen the girder and used for laterally post-tensioning. Hollow girder utilization is a cost-effective option for long-span prestressed concrete bridges because of consuming a reduced amount of material compared to other PC-girders, having a lightweight and spanning long distances⁽²⁰⁾. Figure 1 shows a real hollow PC-girder in which horizontal end cracks have occurred. Observations showed that girders having cracks resulting during the manufacturing stage might cause increased maintenance costs throughout the bridge's life cycle^(21,22).

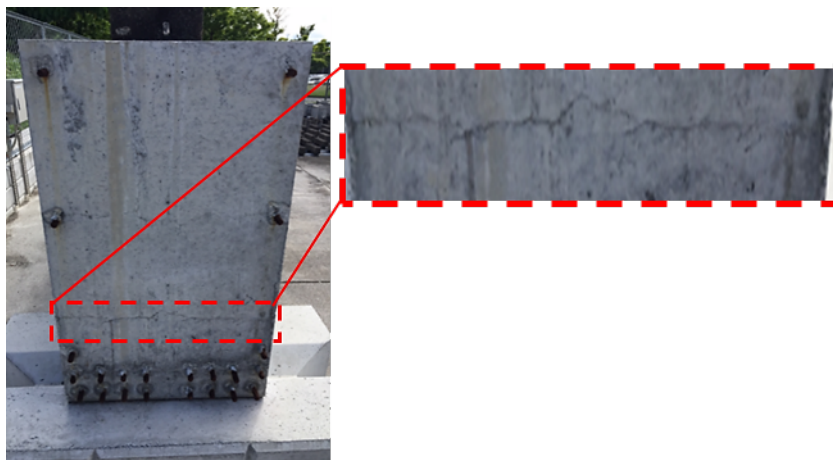


Fig 1. Horizontal cracks at the end of pretensioned hollow PC-girder

In the pretensioning method, first, the tension applies to PC-strand, and the strand becomes slightly thinner than the original thickness; after that, concrete to be poured. The prestress application starts once concrete gets its 70% of strength by releasing strands. At this time, the strand attempts to expand outward to get its original thickness, but concrete does not allow the strand to expand⁽²³⁾, as shown in Figure 2. This phenomenon leads concrete to crack horizontally at the end regions of the girder. Due to bond effects, compressive stresses radiate from strands into the concrete. Therefore, a zone of compressive stresses develops acting radially towards the strands; the dispersion of these compressive stresses causes tensile stresses (principal stresses) to develop normal to the direction of prestressing forces⁽²⁴⁾. If the magnitude of these principal stresses exceeds the tensile strength of concrete, horizontal end cracks occur.

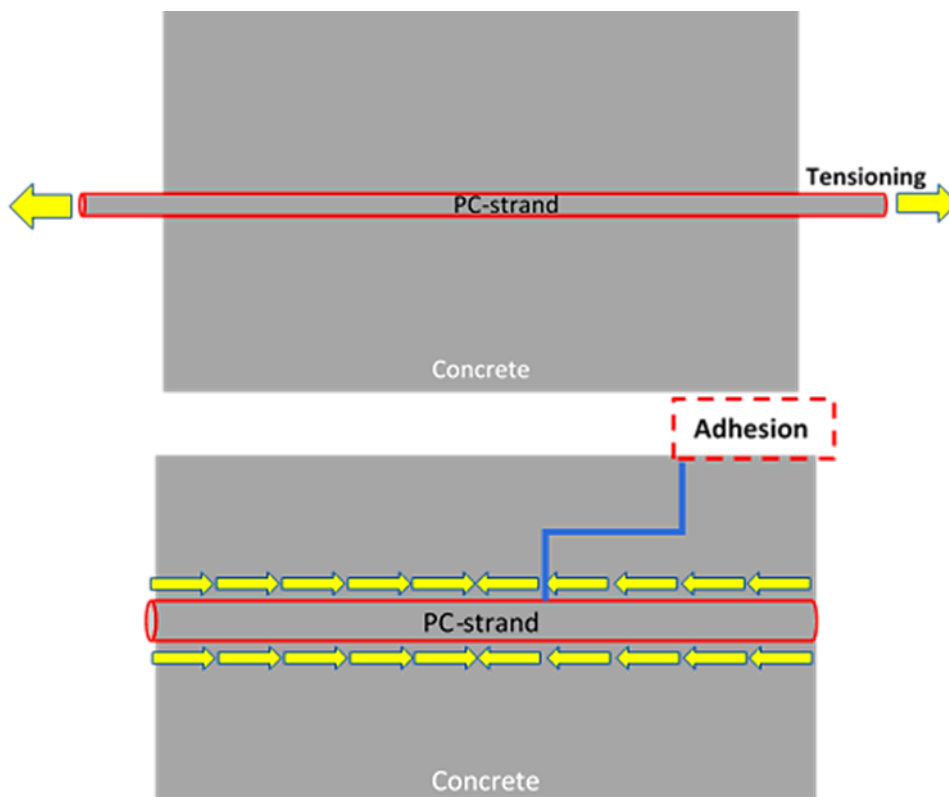


Fig 2. Adhesion occurrence in PC-strand during pretensioning

This study’s main objective was to determine that whether only placing end-zone reinforcements or debonding some strands can successfully eliminate horizontal cracks at the ends of BS18 hollow PC-girder or requires the combination of both methods. BS represents the B-live load slab girder, and the number illustrates the span length of the girder. Considering the long span of BS18 girder, a large amount of prestressing need to be applied at the girder ends, this results in the crack formation and increase the number of crack occurring points. The most common method to reduce principal stresses at the girder ends is designing end-zone reinforcements^(5-7,15,25,26). The American Association of State Highway and Transportation Officials’ AASHTO LRFD Bridge Design Specifications⁽²⁷⁾ section 5.10.10 necessitates end-zone reinforcements to control bursting and splitting stresses. End-zone reinforcements are useful to control the size of cracks but not sufficient for crack elimination⁽²⁸⁾. Debonding some strands in the girder’s end region has been recognized as the most beneficial solution to be effective in reducing principal stresses and can eliminate horizontal end cracks^(6,8,28,29). Hence, the strand-debonding method was applied alongside the end-zone reinforcements to eliminate horizontal cracks at the ends of the BS18 hollow PC-girder.

For simulating the BS18 girder, author used Midas FEA software as the Finite Element Analysis (FEA) software. It is challenging to create a representative finite element model of a prestressed concrete girder through any FEA software^(30,31). Selection of an appropriate constitutive model for concrete, particularly in tension, reasonably simulating the mechanism of stress transfer between strands and concrete, choosing appropriate values for bond stress and the threshold value of slippage, simulating the cracks and their effects in redistributing stresses, and incorporating the interaction of reinforcement steel with concrete are challenging during the simulation. This study utilized nonlinear finite element analysis to evaluate the stress and strain distributions at the ends of hollow PC-girders during and shortly after prestressing.

2 BS18 girder properties

BS18 girder is 18 000 mm (18 m) long with 700 mm height and 700 mm width. This girder uses 16 PC-strands organized into three horizontal rows in the cross-section. The girder is entirely hollow except having six transverse diaphragms to form stiffened the girder. According to JIS A 5373 standards⁽³²⁾, steel reinforcement or stirrup spacings vary throughout the girder’s

length, as shown in Figure 3 . Since steel reinforcements support the girder in carrying loads after the cracking occurs, the stirrups' spacing decreased at the girder's ends.

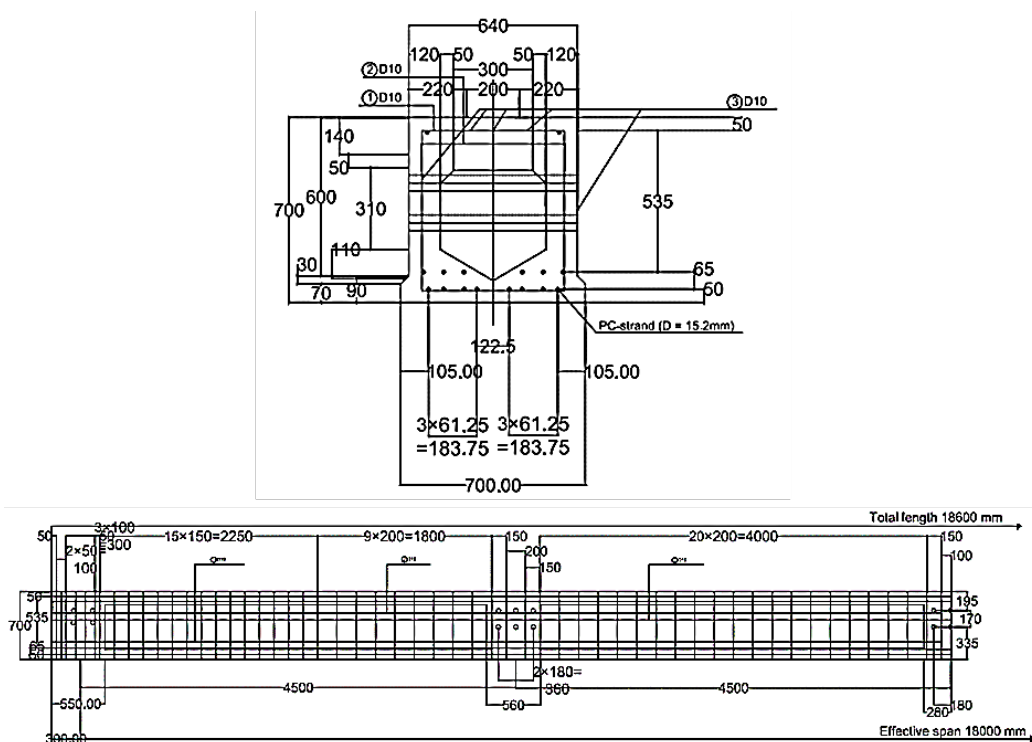


Fig 3. Design dimensions and steel reinforcement details of BS18 girder (32)

3 Numerical analysis

Nonlinear FEA of concrete cracking simulation of a girder with 18 m length can be computationally expensive in time and storage space (20). Thus, for efficient computations, the selected hollow PC-girder was first miniaturized to a 4 m span length to be capable of sufficiently prestressing. Furthermore, considering symmetry in the applied loading and geometry of the miniaturized BS18 girder, half portion of the girder was simulated, and different parts of the model are shown in Figure 4.

The nonlinear analysis was carried out using the structural analysis software Midas FEA. This software is an analysis tool with standard FEM analysis functions in the construction field and can perform detailed analysis to analyze the concrete cracking.

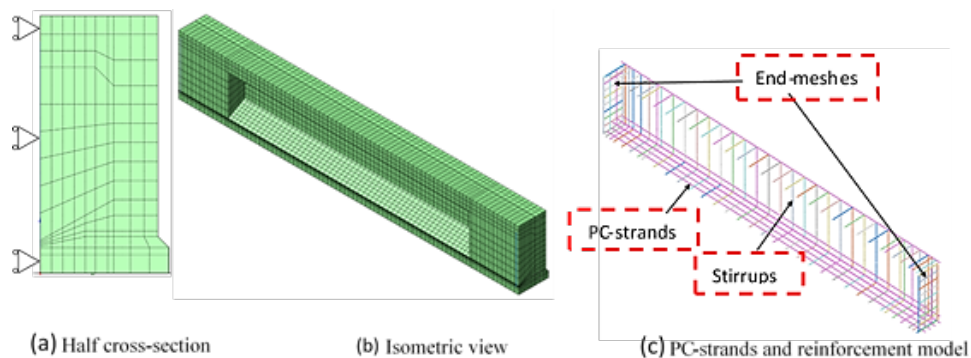


Fig 4. BS18 girder analysis models with 4 m length

3.1 Constitutive laws

This study used the smeared crack approach in which the stresses and strains of concrete and steel were evaluated by average or smeared values crossing several cracks. Total Strain Crack Model (Rotating Crack Model) was utilized to model the concrete behavior. Hordijk and Parabolic functions were used to model the concrete in tension and compression, respectively. The Von Mises model was used to model PC-strands and steel reinforcement bars. Based on the pre-analysis results⁽³³⁾, bond stress and the threshold value of slippage for PC-strands are assumed to be 5.0 N/mm² and 0.2 mm, respectively. Constitutive laws of some materials used in this analysis are shown in Figure 5 .

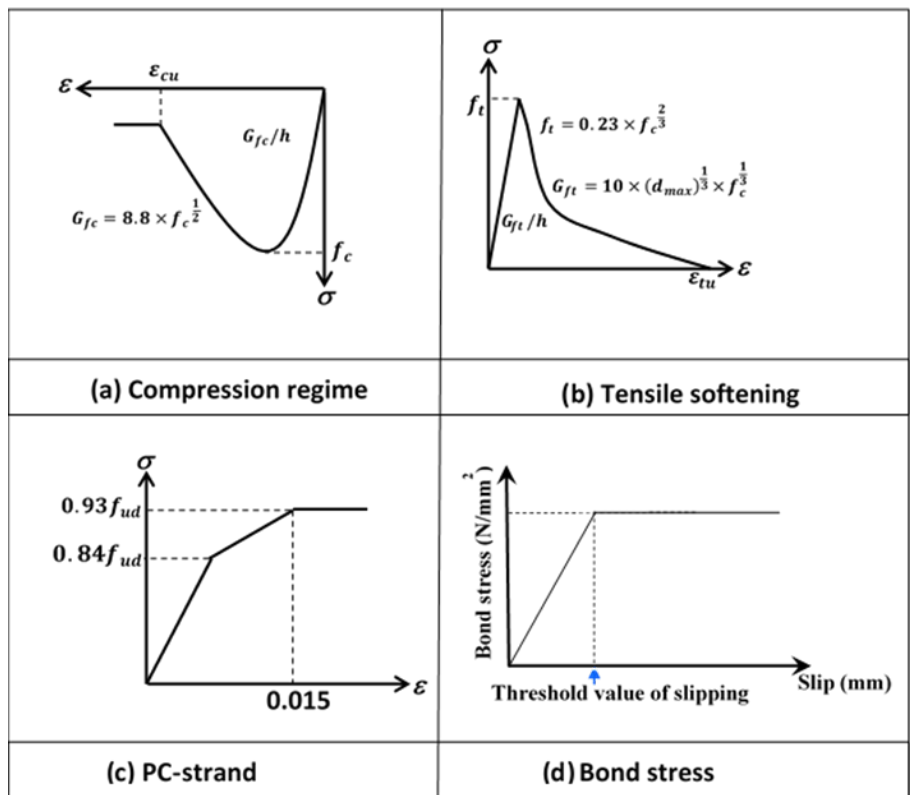


Fig 5. Constitutive laws utilized in the girder modeling

In Figure 5, f_c and f_t show the concrete compressive and tensile strength, respectively, G_{fc} and G_{ft} represent compressive and tensile fracture energy, respectively, ϵ_{cu} and ϵ_{tu} denote the ultimate strain of concrete in compression and in tension, respectively, h is the characteristic element length, d_{max} is the maximum size of coarse aggregate, and f_{ud} is the design tensile strength of PC-strands. The values selected for h and d_{max} in this study are 40.34 mm and 20 mm, respectively.

3.2 Material properties

3.2.1 Concrete

The compressive strength of concrete at the prestressing time was selected 35 N/mm² as per JIS A 5373⁽³²⁾. Other material properties of concrete were obtained using the concrete compressive strength from the following equations⁽³⁴⁾ and are given in Table 1.

$$\text{Tensile strength: } f_t = 0.23 \times f_c^{\frac{2}{3}} \tag{1}$$

$$\text{Tensile fracture energy : } G_t = 10 \times d_{max}^{\frac{1}{3}} \times f_c^{\frac{1}{3}} \tag{2}$$

$$\text{Compressive fracture energy: } G_c = 8.8 \times f_c^2 \tag{3}$$

Table 1. Concrete material properties of BS18 girder model

Analysis Type	Material Properties							
	Compressive Strength (N/mm ²)	Tensile strength (N/mm ²)	Modulus of Elasticity (GPa)	Compressive fracture energy (N/mm)	Tensile fracture energy (N/mm)			
Prestressing	35	2.46	29.5	52.1	0.1			

3.2.2 PC-strands

This study’s strand type is SWPR7BL⁽³⁵⁾, whose modulus of elasticity is 200 000 N/mm², diameter and cross-section area of each strand is 15.2 mm and 138.7 mm², respectively. The Japan Road Association (JRA) Specifications for concrete bridges⁽³⁶⁾ state that the transfer length should be 65 times the strand diameter. The calculated transfer length for the 15.2 mm diameter strand from this relationship is 988 mm. The allowable stress level for prestressing is 1440 N/mm², some relaxations occur after prestressing⁽³²⁾, and it reduces to 1295 N/mm². After detensioning, axial force transfers to concrete, and pretensioning stress decreases to 1110 N/mm² in strands.

3.2.3 Reinforcement Bars

It is stated by AASHTO LRFD Bridge Design Specifications⁽²⁷⁾, vertical reinforcements at the girder ends should not be designed for stresses beyond 138 N/mm². The primary finite element models also specify this, stresses which the reinforcement bars carry are far below their yielding stress. The constitutive model of steel reinforcements used in this study is shown in Figure 6. This model is an Elastic-Perfectly Plastic model and requires only an initial yield condition.

SD295 type reinforcement bars used in this study; their modulus of elasticity is 200 000 N/mm². The reinforcement bars and concrete interaction is considered the reinforcements’ stiffness adds to the continuum elements’ stiffness (Concrete) in which the reinforcements are located. The added ductility of the concrete after cracking is provided by the reinforcement bars. Once concrete elements reach their cracking limit, their load-carrying capacity drops with increasing deformations, larger loads are then transferred to the steel bars. The degrees of freedom of the bar and concrete elements are the same, and the stresses will be distributed to the surrounding bar elements once the concrete elements soften. Since the concrete material’s tension stiffness is too small, even small tension can cause local cracking failure, leading to temporary instability and eventually to convergence problems.

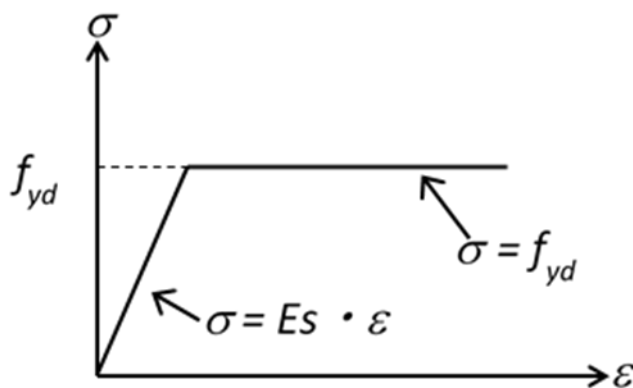


Fig 6. Constitutive model of the used steel reinforcements

3.3 Finite element type and order

Three-dimensional hexahedral elements were used to model concrete, loading plate, and supports in the nonlinear analysis. These elements are an appropriate type of solid elements that are quite practical in modeling arbitrary shapes while an arbitrary mesh is required. Steel reinforcement bars were created as "Embedded Reinforcement Bar Element." In this concept, the reinforcements' stiffness adds to the continuum elements' stiffness in which the reinforcements are located. PC-strands were created as 2-node linear three-dimensional truss elements. A truss element transmits only axial forces and may combine with tension-only/compression-only functions⁽³⁷⁾. Compressive forces were applied to truss elements as prestressing forces.

3.4 Bond Stress

In pretensioned girders, total prestressing forces transfer to concrete by the bond between the prestressing strand and the surrounding concrete^(38,39). Bond stress is shear stress acting parallel to PC-strand's axis on the surface between PC-strand and concrete⁽⁴⁰⁾. Bond slip is the relative displacement between PC-strand and concrete⁽⁴¹⁾. Prestressed concrete depends on the combined action of concrete and its PC-strands for satisfactory operation as a construction material. For this model, bond stress and the threshold value of slipping were adopted as 5.0 N/mm^2 and 0.2 mm , respectively. The constitutive model of bond-slip is illustrated in Figure 5(d).

3.4.1 PC-strands' bond behavior

The bond between PC-strand and concrete can be attributed to adhesion, mechanical interlock, and friction, depending upon the stage of bond development and the nature of the strand's surface. It is essential to evaluate the bonding mechanism simulation with a 3D strand. The strand geometry was modeled as a circular rod, and contact interaction definitions were used to simulate bond behavior. In reality, a strand expands in the radial direction due to Poisson's ratio once prestress is released. This expansion is thought to be one of the possible reasons for end cracking in concrete girders. Evaluating the 3D bond behavior of PC strands thus requires simulation of the strand as a three-dimensional object to simulate its radial interaction with the surrounding concrete. The strand's actual shape is a bundle of seven twisted wires, as shown in Figure 7. It is the helical shape of the twisted pitch that provides the mechanical interlock component for bonding. Modeling such geometry leads to many complications in the numerical simulation of contact interaction between the strand and concrete surfaces. Thus, the strand geometry was simplified to a circular cross-section with an equal area as the actual 7-wire strand. Since the mechanical interlock component to bond resistance cannot be explicitly simulated by modeling the strand as a smooth rod, the interaction property defined between the circular strand and the surrounded concrete includes the effects of adhesion and mechanical interlock. The Poisson's or Hoyer effects automatically include in the simulation by virtue of modeling the strand as a 3D truss element.



Fig 7. PC-strand cross-section used in the model

3.5 Loads

Horizontal cracking occurs immediately after prestressing release when there is no service load on the girder. Therefore, the primary loadings considered for finite element analyses were prestressing forces. Time-dependent effects, such as thermal contraction and creep, were irrelevant during the short interval when cracking occurs. Prestressing loads transfer to girder via bond and friction at the girder ends over a "transfer length" distance. At the girder ends where the strands' slip occurs, stresses in concrete are zero, but concrete carries full effective prestress from strands at the end of the transfer length. As PC-

strands were included in the finite element model as truss elements, prestressing forces were directly applied to the strands. When concrete got 70% of its compressive strength (35 N/mm²), 187.2 KN prestressing force was applied to each strand.

3.6 The Mesh Division

Because of material nonlinearity, the model simulation needs considerable computation time. Finer meshes lead to further accurate results, but the time duration for completing analysis and computations is also a factor in selecting the mesh size. At the ends of the girder, which are the main regions of interest, a finer mesh is expected to provide a much more accurate solution for the inelastic material so that a finer mesh was generated and used for the whole model. The mesh size was selected as 50 mm for this model, as shown in Figure 8.

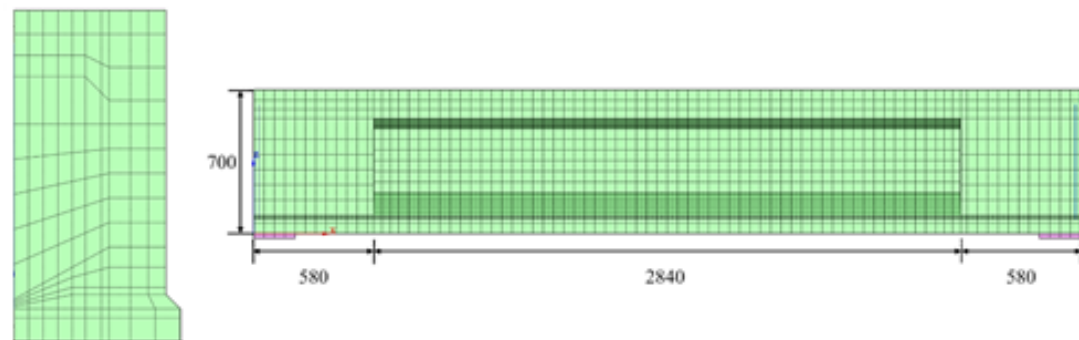


Fig 8. Finite element mesh division used for the model

3.7 Solution Method

In this study, the Iteration method was used as the solution method. FEA solves a set of linear equations at each iteration in the nonlinear analysis. The nonlinear analysis used the “Newton Raphson” method as the solution technique. The relationship between a force vector and displacement vector is no longer linear in the nonlinear analysis. There are many reasons; for example, in the case of material nonlinearity, the relationship becomes nonlinear, and the displacements often depend on the displacements in the earlier stages, e.g., in the case of plastic material behavior⁽³⁷⁾. In linear analysis, the displacement vector should be calculated that equilibrates the internal and external forces, but for determining the equilibrium in the nonlinear case, it is needed not only to make the problems discrete in space (with finite elements) but also in time (with increments)⁽³⁷⁾.

3.8 End-zone reinforcement design

In Case #3 and #4, end-zone reinforcements were placed in both ends of the models. Researchers proposed a design procedure for designing end-zone reinforcements. According to their design procedure⁽²⁵⁾, the following equation was used to obtain the end-zone steel area,

$$A_s = 0.4 \times A_{ps} \tag{4}$$

A_{ps} shows the total prestressing steel area, which is equal to 2496.6 mm² for the BS18 girder. The total steel area computed from Eq. (4) was equal to 988.64.56 mm². The used steel bars in this study were with 10 mm diameter (D10), and the cross-section area of one bar was calculated as 78.5 mm². The number of stirrups to be placed at each end of the girder was 13 bars. The reference⁽²⁵⁾ emphasizes that at least 50 percent of the achieved steel area should be placed within a distance equal to (h/8) from the girder end.

However, placing 6 or 7 stirrups within 87.5 mm length is difficult. Therefore, the designed steel bars were arranged as a mesh pattern, and it is referred to as the end-mesh, as shown in Figure 9(b). The end-mesh was placed 40 mm distant from each end of the girder, as shown in Figure 4 (c).

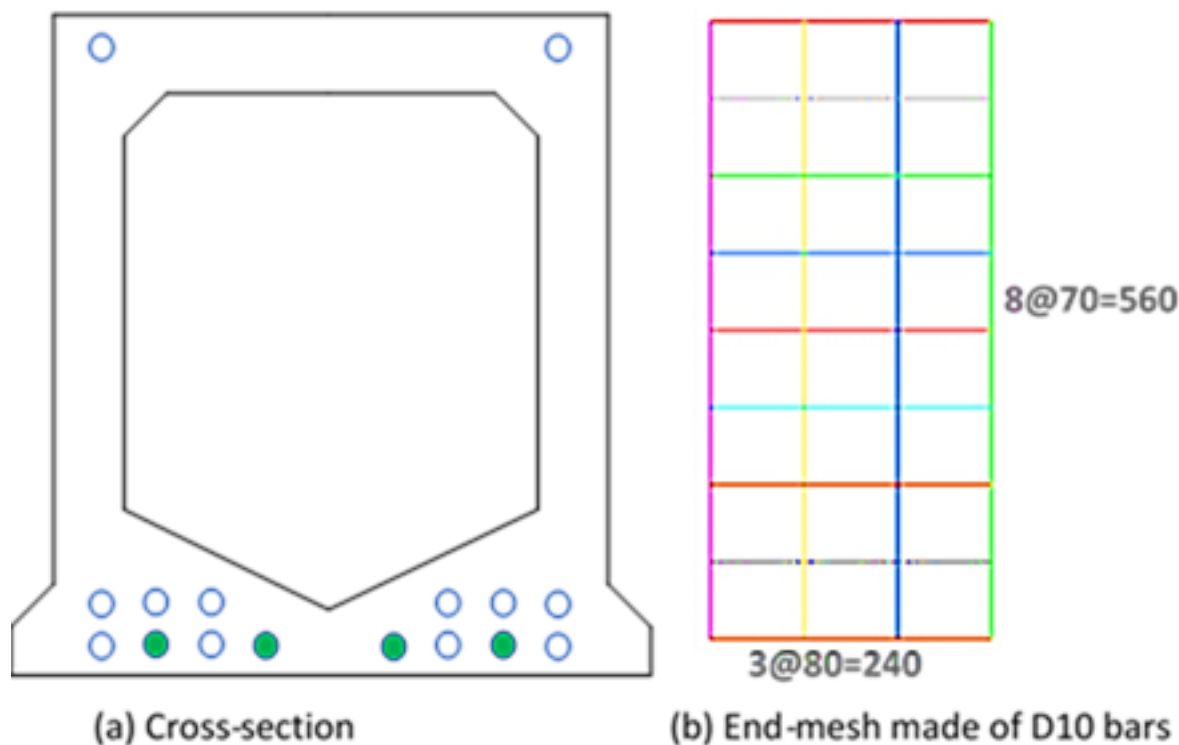


Fig 9. Debonded strand illustration and used end-mesh (○ Debonded strand)

3.9 Analysis cases

Four cases were analyzed for the girder to investigate horizontal end crack occurrences under different conditions, as shown in Table 2. In Case #1, the normal miniaturized BS18 girder was modeled. In Case #2, two PC-strands were debonded for a distance equal to the transfer length at each end of the half model, as shown in Figure 9(a). In Case #3, one end-mesh made of D10 bars (Figure 9(b)) was placed at each end of the girder, as shown in Figure 4 (c). In Case #4, two PC-strands were debonded, and one end-mesh was placed at each end of the model. Principal stress and strain contours were evaluated in each case, and the crack condition was investigated in terms of the principal stress variations in the vertical edge of the girder end.

Additionally, time-based changes of the maximum principal stresses and strains were investigated at the time of prestressing for each case to check that horizontal cracks occur in which percentage of prestressing at the ends of the BS18 girder. Cracking occurs when the maximum principal stresses exceed the tensile strength of concrete. In this work, variations of the principal stresses and strains were studied in four prestressing stages with 5%, 40%, 70%, and 100% prestressing percentages.

Table 2. Analysis cases for the half model

Case	Conditions
1	Fully bonded all PC-strands
2	Debonding two PC-strands
3	Case 1 condition + End-zone reinforcement
4	Case 2 condition + End-zone reinforcement

4 Results

4.1 Temporal changes of principal stresses and strains during prestressing

Temporal changes of the principal stress and strain contours at the ends of the BS18 girder during prestressing for all four cases are shown in Figure 10. Furthermore, Figures 11, 12, 13 and 14 show the maximum principal stress' temporal changes at the

end of the BS18 girder.

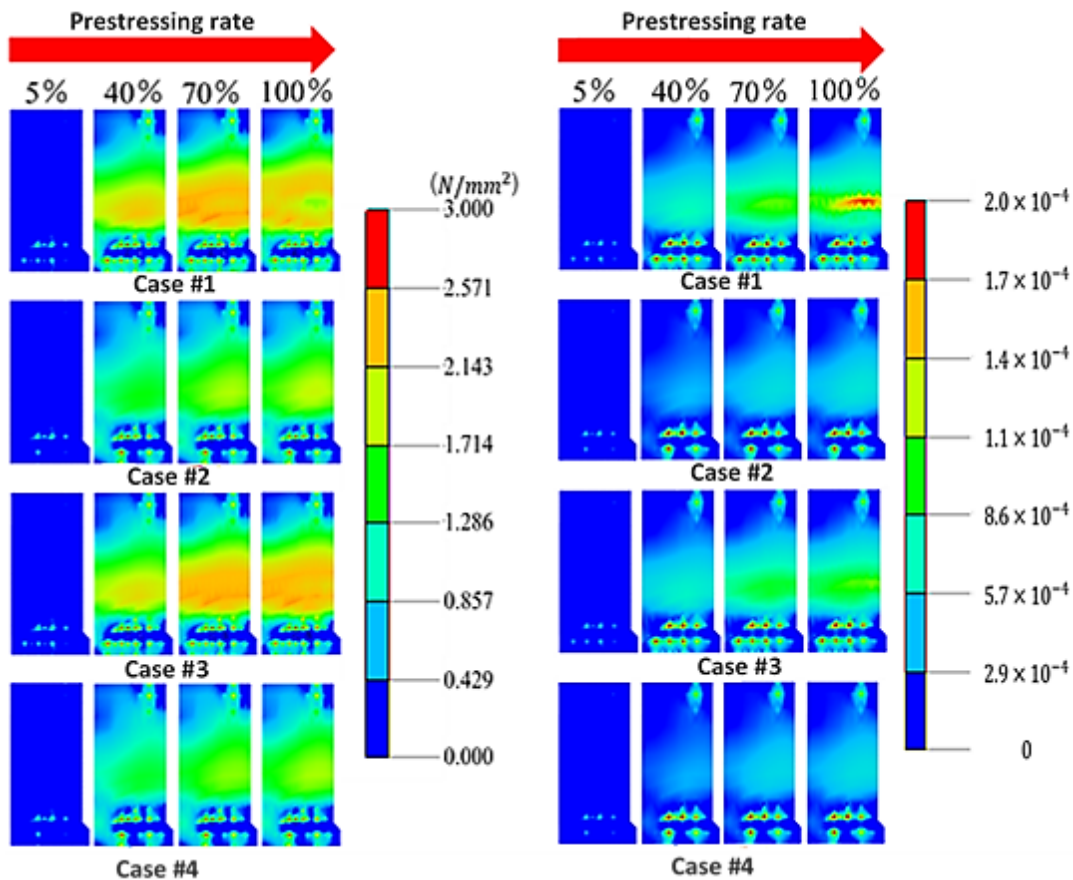


Fig 10. Principal stress contours (left) and principal strain contours (right) for all four cases

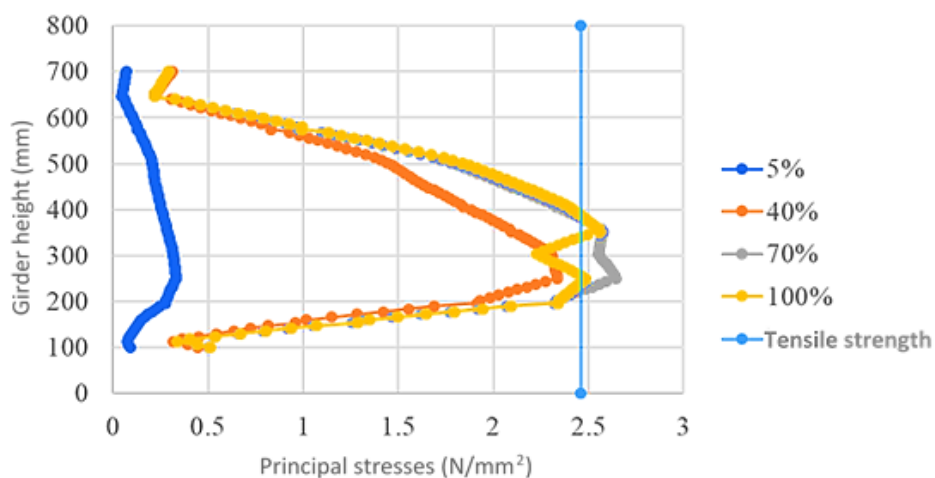


Fig 11. Temporal changes of the principal stresses at the end of the girder (Case #1)

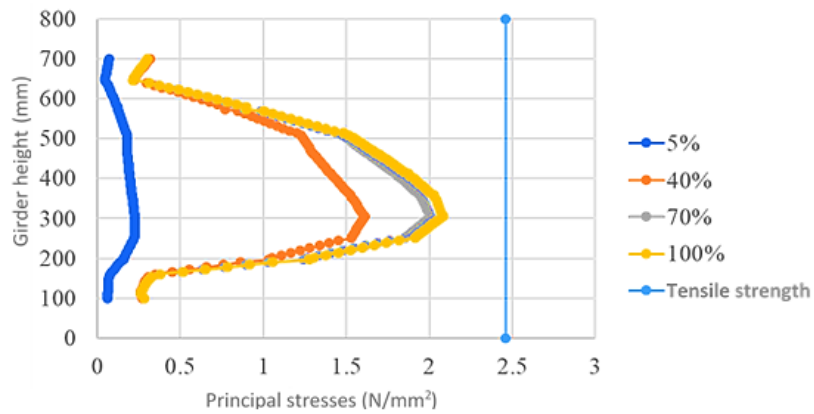


Fig 12. Temporal changes of the principal stresses at the end of the girder (Case #2)

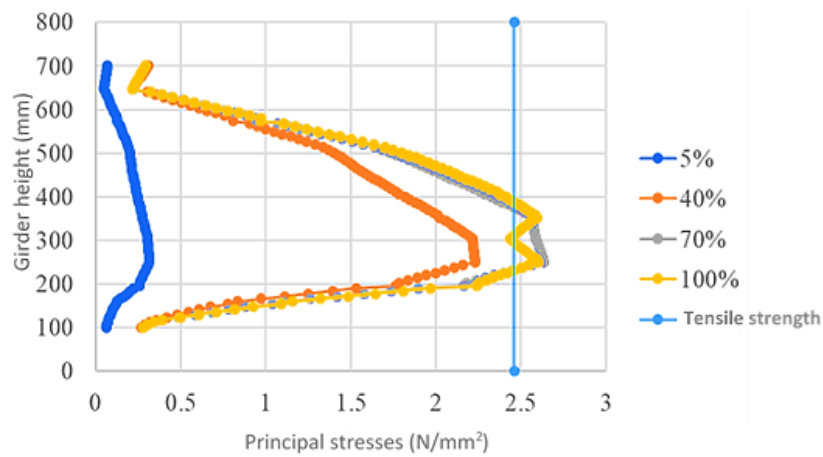


Fig 13. Temporal changes of the principal stresses at the end of the girder (Case #3)

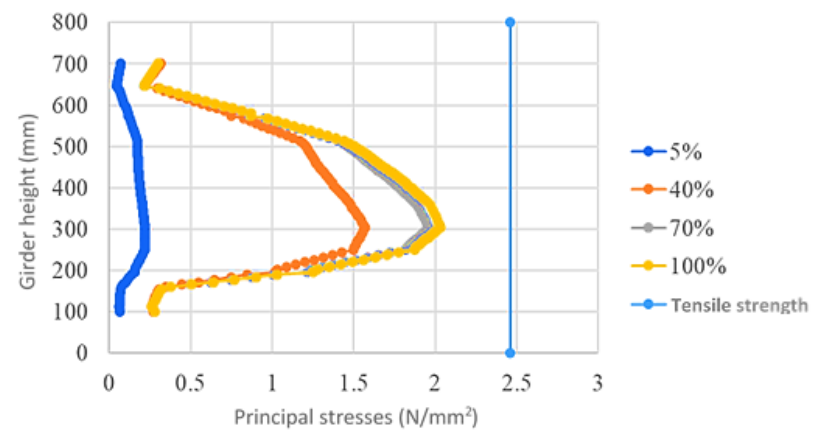


Fig 14. Temporal changes of the principal stresses at the end of the girder (Case #4)

5 Discussion

Figure 11 shows that horizontal cracks occur at the ends of the ordinary BS18 girder model because the magnitude of principal stresses is more than the tensile strength of concrete. In Case #2, debonding two PC-strands in the half model reduced principal stresses to the level to be less than the tensile strength of concrete even in the stage of 100% prestressing as shown in Figure 12, and horizontal cracks are not likely to occur in this case. In Case #3, all PC-strands were fully bonded, and one end mesh was placed at each end of the girder; the magnitude of principal stresses was reduced compared to the stresses in Case #1 but not to the desired level to become less than the tensile strength of concrete as shown in Figure 13, and horizontal cracks are likely to occur in Case #3. In Case #4, two PC-strands were debonded in the half model, and one end-mesh was placed at each end of the girder; principal stresses at the end of the girder for Case #4 are shown in Figure 14. It can be noticed from Figure 14; the magnitude of principal stresses is further reduced to become significantly less than the tensile strength of concrete, and horizontal cracks are eliminated.

6 Conclusion and recommendation

Many researchers studied horizontal cracking at the ends of the ordinary PC-girders. But the methods to prevent horizontal cracks at the ends of the hollow girders are not available in the literature, while hollow beams are incredibly vulnerable to the horizontal end crack occurrence. Thus, in this study, a detailed analytical examination was carried out to propose measures to suppress horizontal cracks at the hollow PC-girder's ends during prestressing. First, prestressing test analysis was performed for four cases with the same material, geometric and other model properties. It was confirmed that horizontal cracks at the ends of the BS18 hollow PC-girder could be suppressed by debonding four PC-strands at the ends of the girder for a distance equal to the transfer length and placing one end-mesh made of D10 bars at each end of the girder.

Followings are the conclusions of this work:

- Numerical analysis illustrated that the magnitude of principal stresses is more than the tensile strength of concrete at the ends of ordinary BS18 girder and horizontal cracks are likely to occur.
- Debonding four PC-strands at the ends of the girder for a distance equal to the transfer length can reduce principal stresses to the level to become less than the tensile strength of concrete, consequently, horizontal end cracks can be eliminated.
- When all PC-strands are fully bonded, placing one end-mesh made of D10 bars at each end of the girder cannot reduce principal stresses to the desired level, and horizontal cracks are likely to occur.
- Combining both methods (Strand-debonding and placing end-zone reinforcements) can further reduce the magnitude of principal stresses to eliminate horizontal end cracks completely.
- Debonding four PC-strands and placing one end-mesh made of D10 bars at each end of the BS18 girder can further reduce principal stresses to a level to be significantly less than the tensile strength of concrete even in the stage of 100% prestressing, and horizontal cracks can be entirely suppressed.
- In this study, horizontal cracks are eliminated at the ends of the BS18 hollow girder with numerical analysis. In the future, it is needed to re-examine these methods through experiments.

References

- 1) Nilson AH. Design of Prestressed Concrete. New York. John Wiley and Sons. 1987.
- 2) Kizilarlan E, Okumus P, Oliva MG. Debonding strands as an anchorage zone crack control method for pretensioned concrete bulb-tee girders. *PCI Journal*. 2020;65(5):65–80. Available from: <https://dx.doi.org/10.15554/pcij65.5-04>.
- 3) Tadros MK, Badie SS, Tuan CY. Transportation Research Board. 2010.
- 4) Maghsoudi M, Maghsoudi AA. Finite Element and Experimental Investigation on the Flexural Response of Pre-tensioned T-Girders. *International Journal of Civil Engineering*. 2019;17(5):541–553. Available from: <https://dx.doi.org/10.1007/s40999-018-0290-3>. doi:10.1007/s40999-018-0290-3.
- 5) Harries KA, Shahrooz BM, Ross BE, Ball P, Trey HR. Modeling and Detailing Pretensioned Concrete Bridge Girder End Regions Using the Strut-and-Tie Approach. *Journal of Bridge Engineering*. 2019;24(3). Available from: [https://dx.doi.org/10.1061/\(asce\)be.1943-5592.0001354](https://dx.doi.org/10.1061/(asce)be.1943-5592.0001354).
- 6) Okumus P, Oliva MG, Becker S. Nonlinear finite element modeling of cracking at ends of pretensioned bridge girders. *Engineering Structures*. 2012;40:267–275. Available from: <https://dx.doi.org/10.1016/j.engstruct.2012.02.033>.
- 7) Okumus P, Kristam RP, Arancibia MD. Sources of Crack Growth in Pretensioned Concrete-Bridge Girder Anchorage Zones after Detensioning. *Journal of Bridge Engineering*. 2016;21(10). Available from: [https://dx.doi.org/10.1061/\(asce\)be.1943-5592.0000928](https://dx.doi.org/10.1061/(asce)be.1943-5592.0000928).
- 8) Meirvenne KV, Corte WD, Boel V, Taerwe L. Non-linear 3D finite element analysis of the anchorage zones of pretensioned concrete girders and experimental verification. *Engineering Structures*. 2018;172:764–779. Available from: <https://dx.doi.org/10.1016/j.engstruct.2018.06.065>. doi:10.1016/j.engstruct.2018.06.065.
- 9) Kannel J, French C, Stolarski H. Release Methodology of Strands to Reduce End Cracking in Pretensioned Concrete Girders. *PCI Journal*. 1997;42(1):42–54. Available from: <https://dx.doi.org/10.15554/pcij.01011997.42.54>.
- 10) Willis M. Post-Tensioning to Prevent End-Region Cracks in Pretensioned Concrete Girders. Clemson, SC. 2014.

- 11) Crispino ED, Cousins TE, Roberts-Wollmann CL. Anchorage zone design for pretensioned precast bulb-T bridge girders in Virginia. *Virginia Center for Transportation Innovation and Research*. 2009.
- 12) Marshall WT, Mattock AH. Control of Horizontal Cracking in the Ends of Pretensioned Prestressed Concrete Girders. *PCI Journal*. 1962;7(5):56–74. Available from: <https://dx.doi.org/10.15554/pcij.10011962.56.74>.
- 13) Gergely P, Sozen MA. Design of Anchorage-Zone Reinforcement in Prestressed Concrete Beams. *PCI Journal*. 1967;12(2):63–75. Available from: <https://dx.doi.org/10.15554/pcij.04011967.63.75>.
- 14) Tan KH, Tong K, Tang CY. Direct Strut-and-Tie Model for Prestressed Deep Beams. *Journal of Structural Engineering*. 2001;127(9):1076–1084. Available from: [https://dx.doi.org/10.1061/\(asce\)0733-9445\(2001\)127:9\(1076\)](https://dx.doi.org/10.1061/(asce)0733-9445(2001)127:9(1076)).
- 15) Arab A, Badie SS, Manzari MT, Khaleghi B, Seguirant SJ, Chapman D. Analytical Investigation and Monitoring of End-Zone Reinforcement of the Alaskan Way Viaduct Super Girders. *PCI Journal*. 2014;59(2):109–128. Available from: <https://dx.doi.org/10.15554/pcij.03012014.109.128>.
- 16) Ronanki VS, Burkhalter DI, Aaleti S, Song W, Richardson JA. Experimental and analytical investigation of end zone cracking in BT-78 girders. *Engineering Structures*. 2017;151:503–517. Available from: <https://dx.doi.org/10.1016/j.engstruct.2017.08.014>.
- 17) Ross BE, Willis MD, Hamilton HR, Consolazio GR. Comparison of details for controlling end-region cracks in precast, pretensioned concrete I-girders. *PCI Journal*. 2014;59(2):96–108. Available from: <https://dx.doi.org/10.15554/pcij.03012014.96.108>.
- 18) O'callaghan MR, Bayrak O. Tensile Stresses in the End Regions of Pretensioned I-Beams at Release. Austin, TX. 2007.
- 19) Karimi AK, Aasim BA, Tomiyama J, Aydan Ö. Control of horizontal cracking at the ends of pretensioned hollow type BS12 PC-girder utilizing FEA. *International Journal of Technical Research and Applications*. 2017;5:63–66.
- 20) Aasim BA, Karimi AK, Tomiyama J, Aydan Ö. Numerical verification of accelerometer-based assessment of hollow-type pretensioned concrete girder. *Asian Journal of Civil Engineering*. 2020;21(3):437–447. Available from: <https://dx.doi.org/10.1007/s42107-019-00219-w>.
- 21) Hasenkamp CJ, Badie, Sameh S, Tuan CY, Tadros, Maher K, et al. Sources of End Zone Cracking of Pretensioned Concrete Girders. In: and others, editor. *Civil Engineering Faculty Proceedings & Presentations*. 2008. Available from: <https://digitalcommons.unomaha.edu/civilengfacproc/5/>.
- 22) Karimi AK, Jaheed AB, Aasim BA, Farooqi JA. Structural Condition and Deficiencies of Present Constructed Bridges over Zahirshahi Canal and Proposal of New Design Using AASHTO Codes. *World Journal of Engineering and Technology*. 2019;07(02):325–332. Available from: <https://dx.doi.org/10.4236/wjet.2019.72023>.
- 23) Prestressed Concrete Engineering Society: Supplementary Revised PC Course for Freshman-Prestressed Concrete (In Japanese language). 2016.
- 24) and RRS. Stresses In The End Zones Of Precast Inverted T-Beams With Tapered Webs. 2018. Available from: https://digitalcommons.wayne.edu/oa_theses/686.
- 25) Tuan CY, Yehia SA, Jongpitaksseel N, Tadros MK. End-zone reinforcement for pretensioned concrete girders. *PCI Journal*. 2004;49(3):68–68. Available from: <https://digitalcommons.unomaha.edu/civilengfacpub/1>.
- 26) Dunkman DA, Hovell CG, Moore AM, Avendano A, Bayrak O, Jirsa JO. Bursting and Spalling in Pretensioned Concrete Beams. In: Third International fib Congress and PCI Annual Convention & Bridge Conference: Proceedings. PCI. 2010.
- 27) AASHTO. American Association of State Highway and Transportation Officials). Washington, DC. AASHTO. .
- 28) Okumus P, Oliva MG. Evaluation of Crack Control Methods for Deep Pretensioned Bridge Girder Ends. *PCI Journal*. 2013.
- 29) Osman M, French C. Debonded Strands in Prestressed Concrete Bridge Girders. 2019.
- 30) Okumus P, Oliva MG. Strand debonding for pretensioned bridge girders to control end cracks. *ACI Structural Journal*. 2014;111(1):201.
- 31) Aasim BA, Karimi AK, Tomiyama J, Aydan Ö. Detection of damage in concrete structure via shifts in natural frequency. *International Journal of Technical Research & Applications*. 2017;5(4):48–52.
- 32) Japanese Industrial Standards (JIS A 5373 - 2010) . .
- 33) Karimi AK, Aasim BA, Tomiyama J, Suda Y, Aydan Ö, Kaneda K. Experimental and numerical studies on the control of horizontal cracking at the ends of hollow-type pretensioned girders. *SN Applied Sciences*. 2020;2(10):1–17. Available from: <https://dx.doi.org/10.1007/s42452-020-03461-z>.
- 34) Standard Specifications for Concrete Structures. Tokyo, Japan. Japan Society of Civil Engineers. 2007.
- 35) Japanese Industrial Standards (JIS G 3536 – 2014) . .
- 36) Japan Road Association. Specification of Highway Bridges, part 3, Concrete Bridges. 2012.
- 37) Finite Element Analysis algorithms. MIDAS FEA. .
- 38) Martí-Vargas JR, Serna P, Navarro-Gregori J, Pallarés L. Bond of 13mm prestressing steel strands in pretensioned concrete members. *Engineering Structures*. 2012;41:403–412. Available from: <https://dx.doi.org/10.1016/j.engstruct.2012.03.056>.
- 39) Ramirez-Garcia AT, Dang CN, Hale WM, Martí-Vargas JR. A higher-order equation for modeling strand bond in pretensioned concrete beams. *Engineering Structures*. 2017;131:345–361. Available from: <https://dx.doi.org/10.1016/j.engstruct.2016.10.050>.
- 40) Sabău M, Pop I, Oneț T. Experimental study on local bond stress-slip relationship in self-compacting concrete. *Materials and Structures*. 2016;49(9):3693–3711. Available from: <https://dx.doi.org/10.1617/s11527-015-0749-5>.
- 41) Casanova A, Jason L, Davenne L. Bond slip model for the simulation of reinforced concrete structures. *Engineering Structures*. 2012;39:66–78. Available from: <https://dx.doi.org/10.1016/j.engstruct.2012.02.007>.